JHEP

Published for SISSA by Springer

Received: *June 9, 2010*
Accepted: *July 12, 2010*
Published: *August 4, 2010*

On the convergence of complex Langevin dynamics: the three-dimensional XY model at finite chemical potential

Gert Aarts and Frank A. James

Department of Physics, Swansea University, Swansea, U.K.

E-mail: g.aarts@swan.ac.uk, pyfj@swan.ac.uk

Abstract: The three-dimensional XY model is studied at finite chemical potential using complex Langevin dynamics. The validity of the approach is probed at small chemical potential using imaginary chemical potential and continuity arguments, and at larger chemical potential by comparison with the world line method. While complex Langevin works for larger β, we find that it fails for smaller β, in the region of the phase diagram corresponding to the disordered phase. Diagnostic tests are developed to identify symptoms correlated with incorrect convergence. We argue that the erroneous behaviour at smaller β is not due to the sign problem, but rather resembles dynamics observed in complex Langevin simulations of simple models with complex noise.

Keywords: Lattice Quantum Field Theory, Lattice QCD

ArXiv ePrint: 1005.3468

doi:10.1007/JHEP08(2010)020

JHEP08(2010)020

Contents

JHEP08(2010)020

1 Introduction

Field theories with a complex action are difficult to treat nonperturbatively, because the weight $e^{-S} = |e^{-S}|e^{i\varphi}$ in the partition function is not real. Standard numerical approaches based on a probability interpretation and importance sampling will then typically break down, which is commonly referred to as the sign problem. This is a pressing problem for QCD at nonzero baryon chemical potential, where a nonperturbative determination of the phase diagram in the plane of temperature and chemical potential is still lacking [1]. Several methods have been developed to explore at least part of the phase diagram [2–19], but in general these can only be applied in a limited region. Recent years have also seen an intense study of the sign problem in QCD and related theories, which has led to new formulations [20, 21] and considerable insight into how the complexity of the weight interplays with physical observables [22–32]. Finally, in some theories the sign problem can be eliminated completely, using a reformulation which yields a manifestly real and positive weight [33–36]. This demonstrates that the sign problem is not a problem of principle for a theory, but instead tied to the formulation and/or algorithm. For QCD an exact reformulation without a sign problem has unfortunately not (yet) been found.

Complex Langevin dynamics [37, 38] offers the possibility of a general solution to this problem. In this formulation the fields, denoted here collectively as ϕ, are supplemented with an additional fictional Langevin time ϑ and the system evolves according to the stochastic equation,

$$\frac{\partial \phi_x(\vartheta)}{\partial \vartheta} = -\frac{\delta S[\phi;\vartheta]}{\delta \phi_x(\vartheta)} + \eta_x(\vartheta). \tag{1.1}$$

In the case that the action is complex, the fields are *complexified* as

$$\phi \to \phi^{\mathrm{R}} + i\phi^{\mathrm{I}}, \tag{1.2}$$

and the Langevin equations read (using general complex noise)

$$\frac{\partial \phi_x^{\mathrm{R}}}{\partial \vartheta} = K_x^{\mathrm{R}} + \sqrt{N_{\mathrm{R}}}\eta_x^{\mathrm{R}}, \qquad K_x^{\mathrm{R}} = -\mathrm{Re}\frac{\delta S}{\delta \phi_x}\Big|_{\phi\to\phi^{\mathrm{R}}+i\phi^{\mathrm{I}}}, \tag{1.3a}$$

$$\frac{\partial \phi_x^{\mathrm{I}}}{\partial \vartheta} = K_x^{\mathrm{I}} + \sqrt{N_{\mathrm{I}}}\eta_x^{\mathrm{I}}, \qquad K_x^{\mathrm{I}} = -\mathrm{Im}\frac{\delta S}{\delta \phi_x}\Big|_{\phi\to\phi^{\mathrm{R}}+i\phi^{\mathrm{I}}}. \tag{1.3b}$$

The strength of the noise in the real and imaginary components of the Langevin equation is constrained via $N_{\mathrm{R}} - N_{\mathrm{I}} = 1$, and the noise furthermore satisfies

$$\langle \eta_x^{\mathrm{R}}(\vartheta)\rangle = \langle \eta_x^{\mathrm{I}}(\vartheta)\rangle = \langle \eta_x^{\mathrm{R}}(\vartheta)\eta_y^{\mathrm{I}}(\vartheta')\rangle = 0, \tag{1.4a}$$

$$\langle \eta_x^{\mathrm{R}}(\vartheta)\eta_y^{\mathrm{R}}(\vartheta')\rangle = \langle \eta_x^{\mathrm{I}}(\vartheta)\eta_y^{\mathrm{I}}(\vartheta')\rangle = 2\delta_{xy}\delta(\vartheta-\vartheta'), \tag{1.4b}$$

i.e., it is Gaussian. Since the complex action is only used to generate the drift terms but not for importance sampling, complex Langevin dynamics can potentially avoid the sign problem.[1]

In the limit of infinite Langevin time, noise averages of observables should equal the standard quantum expectation values. For a real action/Langevin dynamics, formal proofs that observables converge to the correct value can be formulated, using properties of the associated Fokker-Planck equation [45]. If the action is complex and the Langevin dynamics extends into the expanded complexified space, these proofs no longer hold. Nevertheless, a formal derivation of the validity of the approach can still be given, employing holomorphicity and the Cauchy-Riemann equations. We sketch here the basic notion, suppressing all indices for notational simplicity, and refer to ref. [53] for details.

Associated with the Langevin process (1.3) is a (real and positive) probability density $P[\phi^{\mathrm{R}}, \phi^{\mathrm{I}}; \vartheta]$, which evolves according the Fokker-Planck equation

$$\frac{\partial P[\phi^{\mathrm{R}}, \phi^{\mathrm{I}}; \vartheta]}{\partial \vartheta} = L^T P[\phi^{\mathrm{R}}, \phi^{\mathrm{I}}; \vartheta], \tag{1.5}$$

with the Fokker-Planck operator

$$L^T = \frac{\partial}{\partial \phi^{\mathrm{R}}}\left[N_{\mathrm{R}}\frac{\partial}{\partial \phi^{\mathrm{R}}} - K^{\mathrm{R}}\right] + \frac{\partial}{\partial \phi^{\mathrm{I}}}\left[N_{\mathrm{I}}\frac{\partial}{\partial \phi^{\mathrm{I}}} - K^{\mathrm{I}}\right]. \tag{1.6}$$

Stationary solutions of this Fokker-Planck equation are only known in very special cases [41, 51, 53, 56]. Expectation values obtained by solving the stochastic process should then equal

$$\langle O\rangle_{P(\vartheta)} = \frac{\int D\phi^{\mathrm{R}} D\phi^{\mathrm{I}}\, P[\phi^{\mathrm{R}}, \phi^{\mathrm{I}}; \vartheta] O[\phi^{\mathrm{R}} + i\phi^{\mathrm{I}}]}{\int D\phi^{\mathrm{R}} D\phi^{\mathrm{I}}\, P[\phi^{\mathrm{R}}, \phi^{\mathrm{I}}; \vartheta]}. \tag{1.7}$$

However, we may also consider expectation values with respect to a complex weight $\rho[\phi; \vartheta]$,

$$\langle O\rangle_{\rho(\vartheta)} = \frac{\int D\phi\, \rho[\phi; \vartheta] O[\phi]}{\int D\phi\, \rho[\phi; \vartheta]}, \tag{1.8}$$

[1] Early studies of complex Langevin dynamics can be found in, e.g., refs. [39–44]. Ref. [45] contains a further guide to the literature. More recent work includes refs. [46–55].

JHEP08(2010)020

where, using eq. (1.1), ρ evolves according to a complex Fokker-Planck equation

$$\frac{\partial \rho[\phi;\vartheta]}{\partial \vartheta} = L_0^T \rho[\phi;\vartheta], \qquad L_0^T = \frac{\partial}{\partial \phi}\left[\frac{\partial}{\partial \phi} + \frac{\partial S}{\partial \phi}\right]. \tag{1.9}$$

This equation has the desired stationary solution $\rho[\phi] \sim \exp(-S)$.

Under some assumptions and relying on holomorphicity and partial integration [53], one can show that these expectation values are equal, and

$$\langle O \rangle_{P(\vartheta)} = \langle O \rangle_{\rho(\vartheta)}. \tag{1.10}$$

If it can subsequently be shown that

$$\lim_{\vartheta \to \infty} \langle O \rangle_{\rho(\vartheta)} = \langle O \rangle_{\rho(\infty)}, \qquad \rho(\phi;\infty) \sim \exp(-S), \tag{1.11}$$

the applicability of complex Langevin dynamics is demonstrated. In ref. [53] this proposal was studied in some detail in the case of simple models. Remarkably it was found that for complex noise ($N_{\mathrm{I}} > 0$), the Langevin dynamics does *not* converge to the correct answer. On the other hand, for real noise ($N_{\mathrm{I}} = 0$) correct convergence was observed.

In this paper, we continue our investigation into the applicability of complex Langevin dynamics at finite chemical potential [49–53]. We consider the three-dimensional XY model for a number of reasons. We found earlier that this theory is very sensitive to instabilities and runaways and therefore requires the use of an adaptive stepsize [52]. This is similar to the case of QCD in the heavy dense limit [49, 52]. As QCD, this theory has a Roberge-Weiss periodicity at imaginary chemical potential [52, 57]. Furthermore, it is closely related to the relativistic Bose gas at finite chemical potential, for which complex Langevin dynamics was shown to work very well (at weak coupling in four dimensions) [50, 51]. Finally, this theory can be rewritten using a world line formulation without a sign problem [35, 36], which can be solved efficiently using the worm algorithm [36, 58]. This allows for a direct comparison for all parameter values.

The paper is organized as follows. In section 2, we remind the reader of some details of the XY model at real and imaginary chemical potential, the adaptive stepsize algorithm we use and the related phase-quenched XY model. The world line formulation and some properties of the strong-coupling expansion are briefly mentioned in section 3. We then test the validity of complex Langevin dynamics in section 4 and develop diagnostic tests in section 5. In the Conclusion we summarize our findings and discuss possible directions for the future.

2 XY model

The action of the XY model at finite chemical potential is

$$S = -\beta \sum_x \sum_{\nu=0}^{2} \cos(\phi_x - \phi_{x+\hat{\nu}} - i\mu\delta_{\nu,0}), \tag{2.1}$$

JHEP08(2010)020

where $0 \leq \phi_x < 2\pi$. The theory is defined on a lattice of size $\Omega = N_\tau N_s^2$, and we use periodic boundary conditions. The chemical potential μ is coupled to the Noether charge associated with the global symmetry $\phi_x \to \phi_x + \alpha$ and is introduced in the standard way [59]. The action satisfies $S^*(\mu) = S(-\mu^*)$. At vanishing chemical potential the theory is known to undergo a phase transition at $\beta_c = 0.45421$ [36, 60] between a disordered phase when $\beta < \beta_c$ and an ordered phase when $\beta > \beta_c$.

The drift terms appearing in the complex Langevin equations are given by

$$K_x^{\mathrm{R}} = -\beta \sum_\nu \Big[\sin(\phi_x^{\mathrm{R}} - \phi_{x+\hat{\nu}}^{\mathrm{R}}) \cosh(\phi_x^{\mathrm{I}} - \phi_{x+\hat{\nu}}^{\mathrm{I}} - \mu\delta_{\nu,0}) + \sin(\phi_x^{\mathrm{R}} - \phi_{x-\hat{\nu}}^{\mathrm{R}}) \cosh(\phi_x^{\mathrm{I}} - \phi_{x-\hat{\nu}}^{\mathrm{I}} + \mu\delta_{\nu,0}) \Big], \tag{2.2a}$$

$$K_x^{\mathrm{I}} = -\beta \sum_\nu \Big[\cos(\phi_x^{\mathrm{R}} - \phi_{x+\hat{\nu}}^{\mathrm{R}}) \sinh(\phi_x^{\mathrm{I}} - \phi_{x+\hat{\nu}}^{\mathrm{I}} - \mu\delta_{\nu,0}) + \cos(\phi_x^{\mathrm{R}} - \phi_{x-\hat{\nu}}^{\mathrm{R}}) \sinh(\phi_x^{\mathrm{I}} - \phi_{x-\hat{\nu}}^{\mathrm{I}} + \mu\delta_{\nu,0}) \Big]. \tag{2.2b}$$

The equations are integrated numerically by discretizing Langevin time as $\vartheta = n\epsilon_n$ with ϵ_n the adaptive stepsize. Explicitly,

$$\phi_x^{\mathrm{R}}(n+1) = \phi_x^{\mathrm{R}}(n) + \epsilon_n K_x^{\mathrm{R}}(n) + \sqrt{\epsilon_n}\eta_x(n), \tag{2.3a}$$

$$\phi_x^{\mathrm{I}}(n+1) = \phi_x^{\mathrm{I}}(n) + \epsilon_n K_x^{\mathrm{I}}(n), \tag{2.3b}$$

where we specialized to real noise, with $\langle \eta_x(n)\eta_{x'}(n')\rangle = 2\delta_{xx'}\delta_{nn'}$. In the case that $\mu = \phi^{\mathrm{I}} = 0$, the drift terms are bounded and $|K_x^{\mathrm{R}}| < 6\beta$. When $\phi^{\mathrm{I}} \neq 0$, the drift terms are unbounded, which can result in instabilities and runaways. In this particular theory, much care is required to numerically integrate the dynamics in a stable manner and we found that an adaptive stepsize is mandatory [52]. At each timestep, the stepsize is determined according to

$$\epsilon_n = \min\left\{ \bar{\epsilon}, \bar{\epsilon}\frac{\langle K^{\max}\rangle}{K_n^{\max}} \right\}, \tag{2.4}$$

where

$$K_n^{\max} = \max_x \left| K_x^{\mathrm{R}}(n) + iK_x^{\mathrm{I}}(n) \right|. \tag{2.5}$$

Here $\bar{\epsilon}$ is the desired target stepsize and $\langle K^{\max}\rangle$ is either precomputed or computed during the thermalisation phase. All observables are analyzed over equal periods of Langevin time to ensure correct statistical significance.

The observable we focus on primarily in this study is the action density $\langle S\rangle/\Omega$. After complexification the action is written as $S = S^{\mathrm{R}} + iS^{\mathrm{I}}$, with

$$S^{\mathrm{R}} = -\beta \sum_{x,\nu} \cos(\phi_x^{\mathrm{R}} - \phi_{x+\hat{\nu}}^{\mathrm{R}}) \cosh(\phi_x^{\mathrm{I}} - \phi_{x+\hat{\nu}}^{\mathrm{I}} - \mu\delta_{\nu,0}), \tag{2.6a}$$

$$S^{\mathrm{I}} = \beta \sum_{x,\nu} \sin(\phi_x^{\mathrm{R}} - \phi_{x+\hat{\nu}}^{\mathrm{R}}) \sinh(\phi_x^{\mathrm{I}} - \phi_{x+\hat{\nu}}^{\mathrm{I}} - \mu\delta_{\nu,0}). \tag{2.6b}$$

After noise averaging, the expectation value of the imaginary part is consistent with zero while the expectation value of the real part is even in μ, as is expected from symmetry considerations.

JHEP08(2010)020

By choosing an imaginary chemical potential $\mu = i\mu_{\rm I}$ the action (2.1) becomes purely real. This has both the advantage of enabling standard Monte Carlo algorithms to be applied (we choose to employ real Langevin dynamics) and that the behaviour at $\mu^2 \gtrsim 0$ can be assessed by continuation from $\mu^2 \lesssim 0$. The action and drift term with imaginary chemical potential are

$$S_{\rm imag} = -\beta \sum_{x,\nu} \cos(\phi_x - \phi_{x+\hat{\nu}} + \mu_{\rm I}\delta_{\nu,0}), \tag{2.7}$$

$$K_x = -\beta \sum_{\nu} \left[\sin(\phi_x - \phi_{x+\hat{\nu}} + \mu_{\rm I}\delta_{\nu,0}) + \sin(\phi_x - \phi_{x-\hat{\nu}} - \mu_{\rm I}\delta_{\nu,0})\right]. \tag{2.8}$$

This theory is periodic under $\mu_{\rm I} \to \mu_{\rm I} + 2\pi/N_\tau$, which yields a Roberge-Weiss transition at $\mu_{\rm I} = \pi/N_\tau$, similar as in QCD [57]. This periodicity can be made explicit by shifting the chemical potential to the final time slice, via the field redefinition $\phi_{\mathbf{x},\tau} \longrightarrow \phi'_{\mathbf{x},\tau} = \phi_{\mathbf{x},\tau} - \mu_{\rm I}\tau$. The action is then (for arbitrary complex chemical potential)

$$S_{\rm fts} = -\beta \sum_{x,\nu} \cos(\phi_x - \phi_{x+\hat{\nu}} - iN_\tau\mu\delta_{\tau,N_\tau}\delta_{\nu,0}). \tag{2.9}$$

We have also carried out simulations with this action and confirmed the results obtained with the original formulation. The sole exception was the largest β value ($\beta = 0.7$), where the original action missed the Roberge-Weiss transition, while the final-time-slice formulation located it without problems.

The severity of the sign problem is conventionally (see e.g. ref. [1]) estimated by the expectation value of the phase factor $e^{i\varphi} = e^{-S}/|e^{-S}|$ in the phase quenched theory, i.e. in the theory where only the real part of the action (2.1) is included in the Boltzmann weight. In this case, the phase quenched theory is the anisotropic XY model, with the action

$$S_{\rm pq} = -\sum_{x,\nu} \beta_\nu \cos(\phi_x - \phi_{x+\hat{\nu}}), \tag{2.10}$$

where $\beta_0 = \beta\cosh\mu$, and $\beta_{1,2} = \beta$.

3 World line formulation

The advantage of the XY model is that it can be formulated without a sign problem by an exact rewriting of the partition function in terms of world lines [35, 36].[2] Moreover, this dual formulation can be simulated efficiently with a worm algorithm [36, 58], which allows us to compare the results obtained with complex Langevin dynamics with those from the world line approach. We briefly repeat some essential elements of the world line formulation and refer to ref. [36] for more details. The partition function can be rewritten using the identity

$$e^{\beta\cos\phi} = \sum_{k=-\infty}^{\infty} I_k(\beta) e^{ik\phi}, \tag{3.1}$$

[2]The world line formulation has of course a long history in lattice gauge theory, see e.g. ref. [61]. Recent work includes refs. [62–64]. For a review, see ref. [35].

JHEP08(2010)020

where $I_k(\beta)$ are the modified Bessel functions of the first kind. Using this replacement and integrating over the fields, the partition function is written as

$$Z = \int D\phi\, e^{-S} = \sum_{[k]} \prod_{x,\nu} I_{k_{x,\nu}}(\beta) e^{k_{x,\nu}\mu\delta_{\nu,0}} \delta\left(\sum_{\nu} [k_{x,\nu} - k_{x-\hat{\nu},\nu}]\right). \tag{3.2}$$

The sum over $[k]$ indicates a sum over all possible world line configurations. Since $\langle S\rangle = -\beta\frac{\partial \ln Z}{\partial\beta}$, the action can be computed from

$$\langle S\rangle = -\beta \left\langle \sum_{x,\nu} \left[\frac{I_{k_{x,\nu}-1}(\beta)}{I_{k_{x,\nu}}(\beta)} - \frac{k_{x,\nu}}{\beta}\right]\right\rangle_{\rm wl}, \tag{3.3}$$

where the brackets denote the average over world line configurations. To compute this average, we have implemented the worm algorithm, following ref. [36]. We note here, amusingly, that the world line formulation has a sign problem at imaginary chemical potential.

Inspired by ref. [65], we have also studied a (low-order) strong-coupling expansion of this model, using

$$I_k(2x) = \frac{x^k}{k!}\left(1 + \frac{x^2}{k+1} + \frac{x^4}{2(k+2)(k+1)} + \ldots\right). \tag{3.4}$$

At strong coupling the chemical potential cancels in most world lines, except when the world line wraps around the temporal direction. At leading order in the strong-coupling expansion, it then appears in the combination $(\frac{1}{2}\beta e^{\mu})^{N_\tau}$. In the thermodynamic limit it therefore contributes only when $\frac{1}{2}\beta e^{\mu} \geq 1$. Hence a simple strong-coupling estimate for the critical coupling at nonzero μ is given by

$$\beta_c(\mu) = 2e^{-\mu}. \tag{3.5}$$

The μ-independence at small β and μ is known as the Silver Blaze feature in QCD [66].

The partition function is expressed in terms of the free energy density f as $Z = \exp(-\Omega f)$. A strong-coupling expansion to order β^4 on a lattice with $N_\tau > 4$ yields

$$f = -\frac{3}{4}\beta^2 - \frac{21}{64}\beta^4 + \mathcal{O}(\beta^6), \tag{3.6}$$

and hence

$$\langle S\rangle/\Omega = -\frac{3}{2}\beta^2 - \frac{21}{16}\beta^4 + \mathcal{O}(\beta^6). \tag{3.7}$$

In the phase quenched theory we find

$$f_{\rm pq} = -\frac{1}{4}\beta^2\left(2 + \cosh^2\mu\right) - \frac{1}{64}\beta^4\left(14 + 8\cosh^2\mu - \cosh^4\mu\right) + \mathcal{O}(\beta^6). \tag{3.8}$$

We can now estimate the severeness of the sign problem at strong coupling. The average phase factor takes the standard form,

$$\langle e^{i\varphi}\rangle_{\rm pq} = \frac{Z}{Z_{\rm pq}} = \exp\left[-\Omega\Delta f\right], \qquad \Delta f = f - f_{\rm pq}, \tag{3.9}$$

where in this case

$$\Delta f = \frac{1}{4}\beta^2\left(\cosh^2\mu - 1\right) + \frac{1}{64}\beta^4\left(\cosh^2\mu - 1\right)\left(7 - \cosh^2\mu\right) + \mathcal{O}(\beta^6). \tag{3.10}$$

On a finite lattice and for small chemical potential we find therefore the sign problem to be mild in the strong-coupling limit, since the volume factor is balanced by $\beta^2\mu^2/4 \ll 1$.

JHEP08(2010)020

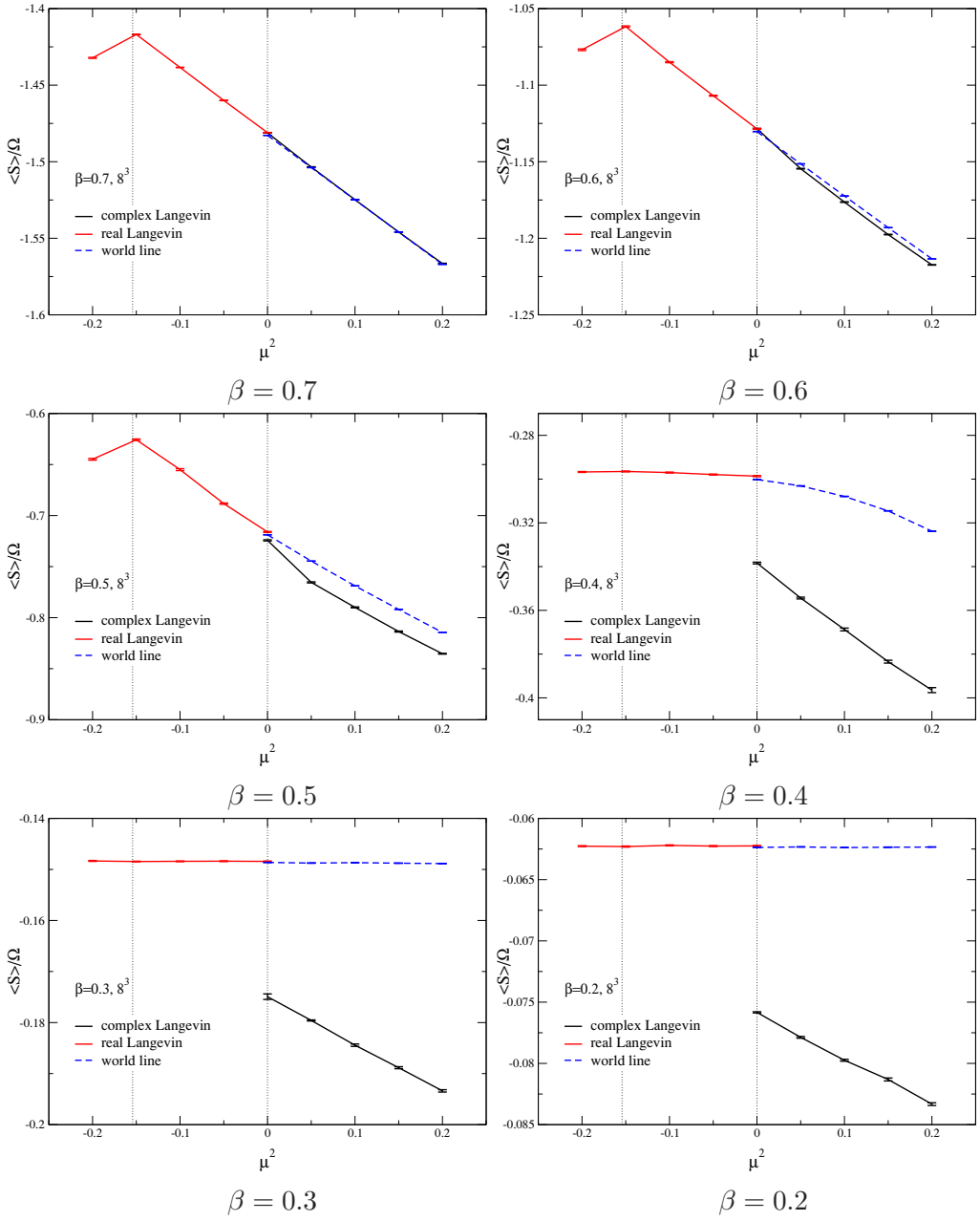

Figure 1. Real part of action density $\langle S\rangle/\Omega$ as a function of μ^2 on a lattice of size 8^3, using complex Langevin dynamics and the world line formulation at real μ ($\mu^2 > 0$) and real Langevin dynamics at imaginary μ ($\mu^2 < 0$). The vertical lines on the left indicate the Roberge-Weiss transitions at $\mu_{\rm I} = \pi/8$.

4 Comparison

We start to assess the applicability of complex Langevin dynamics for this model at small chemical potential. In this case we can use continuity arguments to compare observables at real and imaginary chemical potential. In figure 1 the real part of the action density is

JHEP08(2010)020

shown as a function of μ^2, for several values of β: from the ordered phase at large β to the disordered phase at low β. We observe that at the highest values of β this observable is continuous across $\mu^2 = 0$, which is a good indication that complex Langevin dynamics works well in this region. The cusp at $\mu_{\rm I} = \pi/N_\tau$ (corresponding to $\mu^2 = -0.154$) reflects the Roberge-Weiss transition. At lower β, however, we observe that the action density is no longer continuous: this is interpreted as a breakdown of complex Langevin dynamics. In order to verify this, figure 1 also contains the expectation values of the action density found using the worm algorithm in the world line formalism for real μ. As expected, in this case the action density is continuous across $\mu^2 = 0$ for all values of β, confirming the interpretation given above. We have verified that the jump in the action density at lower β is independent of the lattice volume. We have also verified that the discrepancy at $\mu^2 = 0$ between real Langevin dynamics and the world line result (at e.g. $\beta = 0.4$) is due to the finite Langevin stepsize.

For small β, the numerical results found with the worm algorithm are consistent with those derived analytically in the strong-coupling limit above. The expectation value of the action density is μ independent and hence the Roberge-Weiss periodicity is smoothly realized. Using eq. (3.7), we also find quantitative agreement: in the strong-coupling expansion $\langle S\rangle/\Omega = -0.0621 + \mathcal{O}(10^{-4})$ for $\beta = 0.2$ and $-0.145 + \mathcal{O}(10^{-3})$ for $\beta = 0.3$.

As discussed above, for the parameter values and lattice sizes used here the sign problem is not severe: taking $\mu^2 = 0.1$ and $\beta = 0.2$, we find that

$$\Omega\Delta f \approx \Omega\frac{\beta^2\mu^2}{4} \approx 0.51, \qquad \langle e^{i\varphi}\rangle_{\rm pq} \approx 0.60. \tag{4.1}$$

We take this as a first indication that the observed breakdown is not due to the presence of the sign problem, especially since complex Langevin dynamics has been demonstrated to work well in other models where the sign problem is severe [50, 51].

To probe the reliability of complex Langevin dynamics for larger values of μ, we have computed the action density for a large number of parameter values in the $\beta - \mu$ plane. Our findings are summarized in figure 2, where we show the relative difference between the action densities obtained with complex Langevin (cl) and in the world line formulation (wl), according to

$$\Delta S = \frac{\langle S\rangle_{\rm wl} - \langle S\rangle_{\rm cl}}{\langle S\rangle_{\rm wl}}. \tag{4.2}$$

Also shown in this figure is the phase transition line $\beta_c(\mu)$, taken from ref. [36]. We observe a clear correlation between the breakdown of Langevin dynamics and the phase boundary: complex Langevin dynamics works fine well inside the ordered phase, but breaks down in the boundary region and the disordered phase. The largest deviation around $\mu = 2$ is due to the Silver Blaze effect: the difference between the action density found with complex Langevin dynamics and the correct μ-independent action density is maximal just before crossing over to the other phase, where the agreement improves quickly.

JHEP08(2010)020

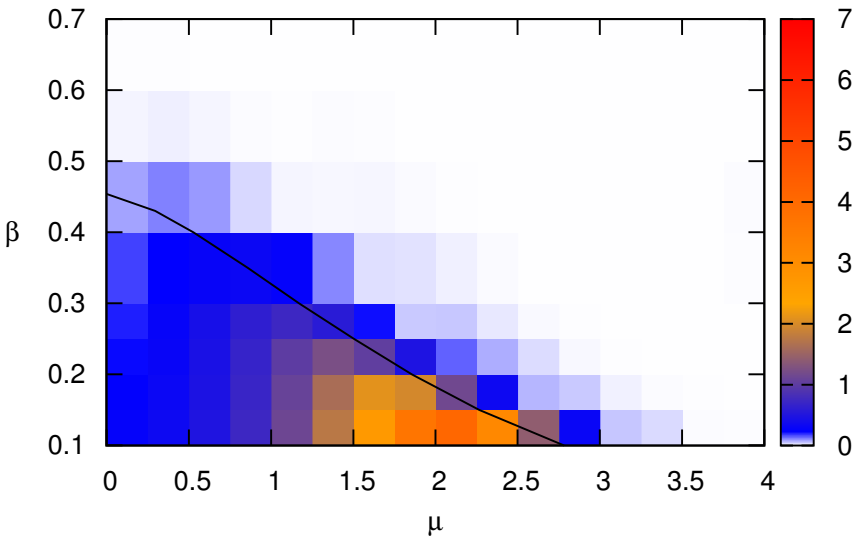

Figure 2. Colour plot indicating the relative difference ΔS between the expectation value of the action density obtained with complex Langevin dynamics and in the world line formulation, see eq. (4.2). Also shown is the phase boundary $\beta_c(\mu)$ between the ordered (large β) and disordered (small β) phase [36].

5 Diagnostics

In this section we attempt to characterize the results presented above in terms of properties of complex Langevin dynamics and the distribution $P[\phi^{\mathrm{R}}, \phi^{\mathrm{I}}]$ in the complexified field space, see eq. (1.7). We suppress Langevin time dependence, since we always consider the quasi-stationary regime, i.e. the initial part of the evolution is discarded (we considered Langevin times up to $\vartheta \sim 2 \times 10^4$). Our aim is to argue that the discrepancy at small β is introduced by complex Langevin dynamics rather than by the presence of a chemical potential and hence not due to the sign problem.

A first test of the validity of complex Langevin dynamics is to compare simulations at $\mu = 0$ using a cold start, i.e. with $\phi^{\mathrm{I}} = 0$ initially, and a hot start in which ϕ^{I} is taken from a Gaussian distribution.[3] When $\mu = 0$, a cold start corresponds to real Langevin dynamics. In the case of a hot start, however, the fields lie immediately in the complexified space and so the dynamics is complexified. Comparison of results obtained with these two initial ensembles gives insight into the inner workings of complex Langevin dynamics. We have computed the expectation value of the action density at $\mu = 0$ using both a hot and a cold start. We found them to agree at large β, despite the fact that the imaginary components of the field are initialised randomly. However, when $\beta \lesssim 0.5$, they disagree. Moreover, the result from the cold start agrees with the one obtained in the world line formulation. One is therefore led to conclude that when $\mu = 0$ the imaginary components ϕ^{I} are driven

[3]The real components ϕ^{R} are taken from a Gaussian distribution always.

JHEP08(2010)020

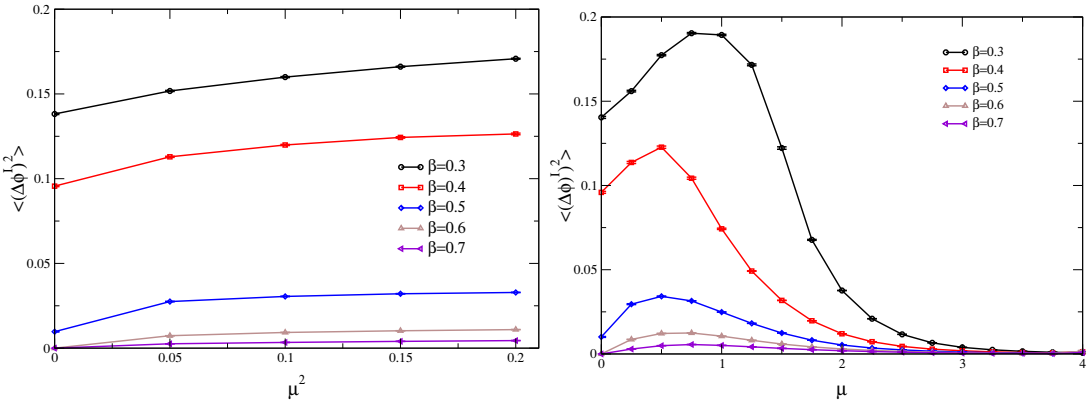

Figure 3. Width of the distribution $P[\phi^{\mathrm{R}}, \phi^{\mathrm{I}}]$ in the imaginary direction for various values of β as a function of μ^2 on a 10^3 lattice (left) and, for larger μ, as a function of μ on a 8^3 lattice (right).

to zero (more precisely, to a constant value) at large β but are not constrained at small β. In other words the drift terms are not capable of restoring the reality of the dynamics. It is tempting to relate this to being in (or close to) the disordered phase. We note that it cannot be understood from the classical fixed point structure, since this is independent of β. We also remark that the dynamics at small β resembles Langevin dynamics with complex noise ($N_{\mathrm{I}} > 0$) [53], where the trajectories are kept in the complexified field space by the stochastic kicks on ϕ^{I} (rather than by the drift terms, as is the case here).

In terms of the distribution $P[\phi^{\mathrm{R}}, \phi^{\mathrm{I}}]$, these findings imply that $P[\phi^{\mathrm{R}}, \phi^{\mathrm{I}}] \sim e^{-S}\delta(\phi^{\mathrm{I}})$ at large β, but not at small β. This can be further investigated by studying the width of the distribution in the imaginary direction,[4]

$$\left\langle \left(\Delta\phi^{\mathrm{I}}\right)^2 \right\rangle = \left\langle \frac{1}{\Omega} \sum_x \left(\phi_x^{\mathrm{I}}\right)^2 \right\rangle - \left\langle \frac{1}{\Omega} \sum_x \phi_x^{\mathrm{I}} \right\rangle^2 . \tag{5.1}$$

When $\mu = 0$ the width should vanish, while when turning on μ one may expect it to increase smoothly. The results are shown in figure 3. For the larger β values this is exactly what is observed: the width increases smoothly from zero. For the smaller β values, however, we observe that the width is nonzero even when $\mu = 0$ (when using a hot start), and remains large for nonzero μ. At larger values of μ the width is driven again towards zero and agreement with the world line results improves, see figure 2. We remark here that it is possible that different distributions (with different widths) yield the same result for observables. This is what is theoretically expected in the presence of complex noise ($N_{\mathrm{I}} \geq 0$) [53] and can be seen analytically in gaussian models with complex noise, where a continuous family of distributions $P[\phi^{\mathrm{R}}, \phi^{\mathrm{I}}; N_{\mathrm{I}}]$ all yield the same result for observables, independent of N_{I}, even though the width of these distributions is nonzero and increases with N_{I} [67]. In the case we study here, however, we find that the failure of complex Langevin dynamics in the disordered phase is correlated with the

[4]The mean value $\langle \phi^{\mathrm{I}} \rangle = 0$; in the large β phase, this requires averaging over a large number of initial conditions.

JHEP08(2010)020

spread of the distribution $P[\phi^{\mathrm{R}}, \phi^{\mathrm{I}}]$ in the noncompact direction. We conclude that a relatively narrow distribution, with a smoothly increasing width, is required. We note again that this resembles observations made in simulations of nongaussian models with complex noise [53, 68].

To investigate the interplay between (the width of) the distribution and observables, we express expectation values as

$$\langle A[\phi^{\mathrm{R}}, \phi^{\mathrm{I}}]\rangle = \frac{1}{Z}\int D\phi^{\mathrm{R}} D\phi^{\mathrm{I}}\, P[\phi^{\mathrm{R}}, \phi^{\mathrm{I}}] A[\phi^{\mathrm{R}}, \phi^{\mathrm{I}}], \tag{5.2}$$

with

$$Z = \int D\phi^{\mathrm{R}} D\phi^{\mathrm{I}}\, P[\phi^{\mathrm{R}}, \phi^{\mathrm{I}}]. \tag{5.3}$$

In general the operator A is not required to be holomorphic, i.e. a function of $\phi^{\mathrm{R}} + i\phi^{\mathrm{I}}$, since this will allow more insight in properties of the distribution.[5] The distribution of an operator A can then be defined according to

$$\langle A\rangle = \int dA\, P(A) A = \frac{1}{Z}\int D\phi^{\mathrm{R}} D\phi^{\mathrm{I}}\, P[\phi^{\mathrm{R}}, \phi^{\mathrm{I}}] A[\phi^{\mathrm{R}}, \phi^{\mathrm{I}}], \tag{5.4}$$

where

$$P(A) = \frac{1}{Z}\int D\phi^{\mathrm{R}} D\phi^{\mathrm{I}}\, P[\phi^{\mathrm{R}}, \phi^{\mathrm{I}}] \delta(A - A[\phi^{\mathrm{R}}, \phi^{\mathrm{I}}]), \tag{5.5}$$

with the normalization

$$\int dA\, P(A) = 1. \tag{5.6}$$

Distributions $P(A)$ can be constructed numerically, by sampling A from configurations generated by complex Langevin dynamics.

The distribution for the action density is shown in figure 4, comparing again a hot and cold start at $\mu = 0$. This figure supports the earlier claim that real and complex Langevin match at larger β but fail at smaller β. However, the reason for failure is somewhat subtle. Naïvely, one might expect a large "tail" caused by excursions in the complexified field space to affect the expectation value but this does not appear to happen. Instead we find that the entire distribution is shifted and becomes only slightly wider at $\beta \lesssim 0.5$ when the hot start is used.

Finally, the observed difference at large and small β also appears prominently in the actual dynamics, i.e. in the drift terms. We have analyzed the maximal force $K^{\max}$ appearing in the adaptive stepsize algorithm. In the case of real Langevin dynamics, the drift terms are limited by an upper bound of $K^{\max} \leq 6\beta$. In the complexified space there is no upper limit and the drift terms can in principle become several orders of magnitude larger [52]. The distribution of $K^{\max}$ is plotted at $\mu = 0$ with hot and cold starts in figure 5. In the large β phase, the distributions appear identical, with $K^{\max} \leq 6\beta$. This is consistent with the conclusion reached above. In the low β phase the distributions are dramatically different: in the complexified dynamics, triggered by the hot start, much larger forces appear. The distributions are no longer peaked but very broad with a long tail (note

[5] Of course only holomorphic functions correspond to observables in the original theory.

JHEP08(2010)020

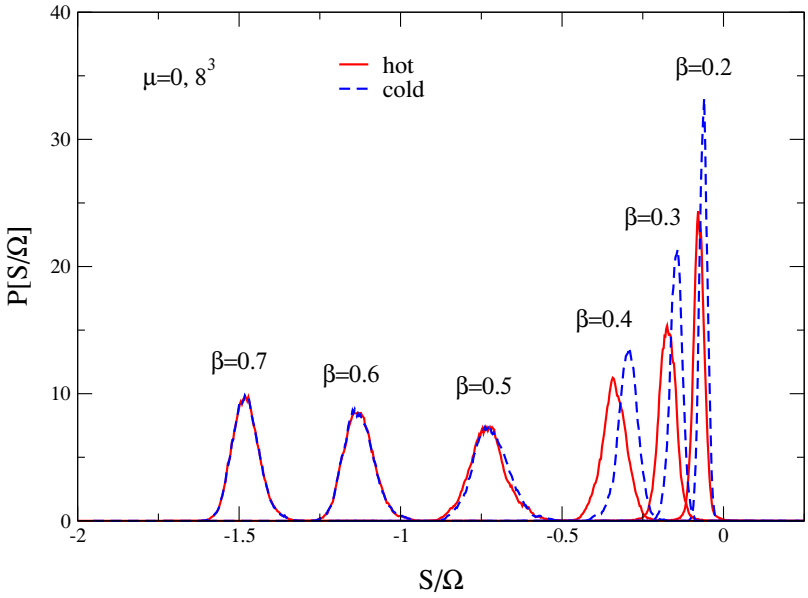

Figure 4. Distribution of action density S/Ω for various values of β at $\mu = 0$ on a 8^3 lattice, using a hot and a cold start.

the horizontal logarithmic scale). At $\beta = 0.5$ we observe interesting crossover behaviour: both the peaked distribution bounded by $K^{\max} = 6\beta$ and a decaying "tail" characteristic of small β distributions appear.

To study the two possible distributions of $K^{\max}$ further, we show in figure 6 the same results but now with $\mu = 0.1$. In this case the hot and cold start yield identical distributions, since both simulations are complexified due to the nonzero chemical potential. The striking difference between the distributions at large and small β is still present. At large β the force can occasionally be large, making the use of an adaptive stepsize necessary. However, the typical value is still determined by the maximal value for real Langevin dynamics, i.e. 6β. At small β this part of the distribution is completely gone and is replaced by a broad distribution at much larger $K^{\max}$ values. Again at $\beta = 0.5$ we observe crossover behaviour with both features present. These results are qualitatively the same on larger volumes.

Let us summarize the findings of this section. Complex Langevin dynamics works well at large β in the ordered phase. The distribution $P[\phi^{\mathrm{I}}, \phi^{\mathrm{I}}]$ in the complexified field space is relatively narrow in the noncompact direction and Langevin simulations started with hot and cold initial conditions agree. The drift terms do occasionally become large but the typical size is set by the maximal value for real Langevin evolution. At small β, in or close to the disordered phase, the distribution is much wider in the ϕ^{I} direction. Typical drift terms are much larger, with a wide spread in the distribution. At $\mu = 0$ complexified dynamics does not reduce to real dynamics. There is a strong correlation with the phase the theory is in (see figure 2), but not with the sign problem, since these observations also hold at $\mu = 0$ and are independent of the lattice volume. Moreover, for the lattice volumes we consider the sign problem is not severe. We emphasize that a firm conclusion can only be drawn after all the findings presented above are combined consistently, while the observation of e.g. large drift terms or a large width by itself would clearly be insufficient.

JHEP08(2010)020

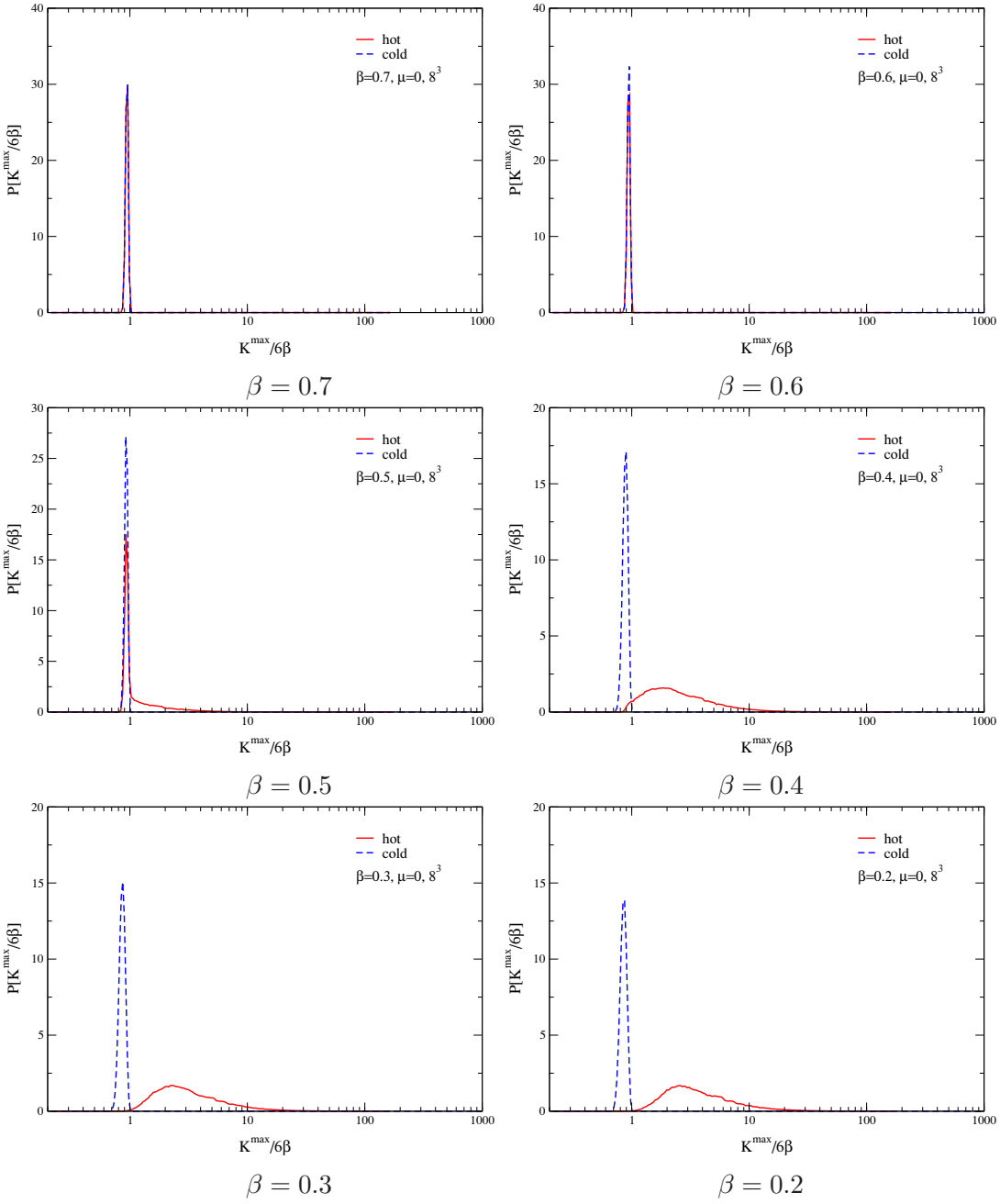

Figure 5. Distribution of $K^{\max}/(6\beta)$ at $\mu = 0$ on a 8^3 lattice using a hot and a cold start.

6 Conclusion

We have studied the applicability of complex Langevin dynamics to simulate field theories with a complex action due to a finite chemical potential, in the case of the three-dimensional XY model. Using analytical continuation from imaginary chemical potential and comparison with the world line formulation we found that complex Langevin dynamics yields reliable results at larger β but fails when $\beta \lesssim 0.5$ at small chemical potential. We estab-

JHEP08(2010)020

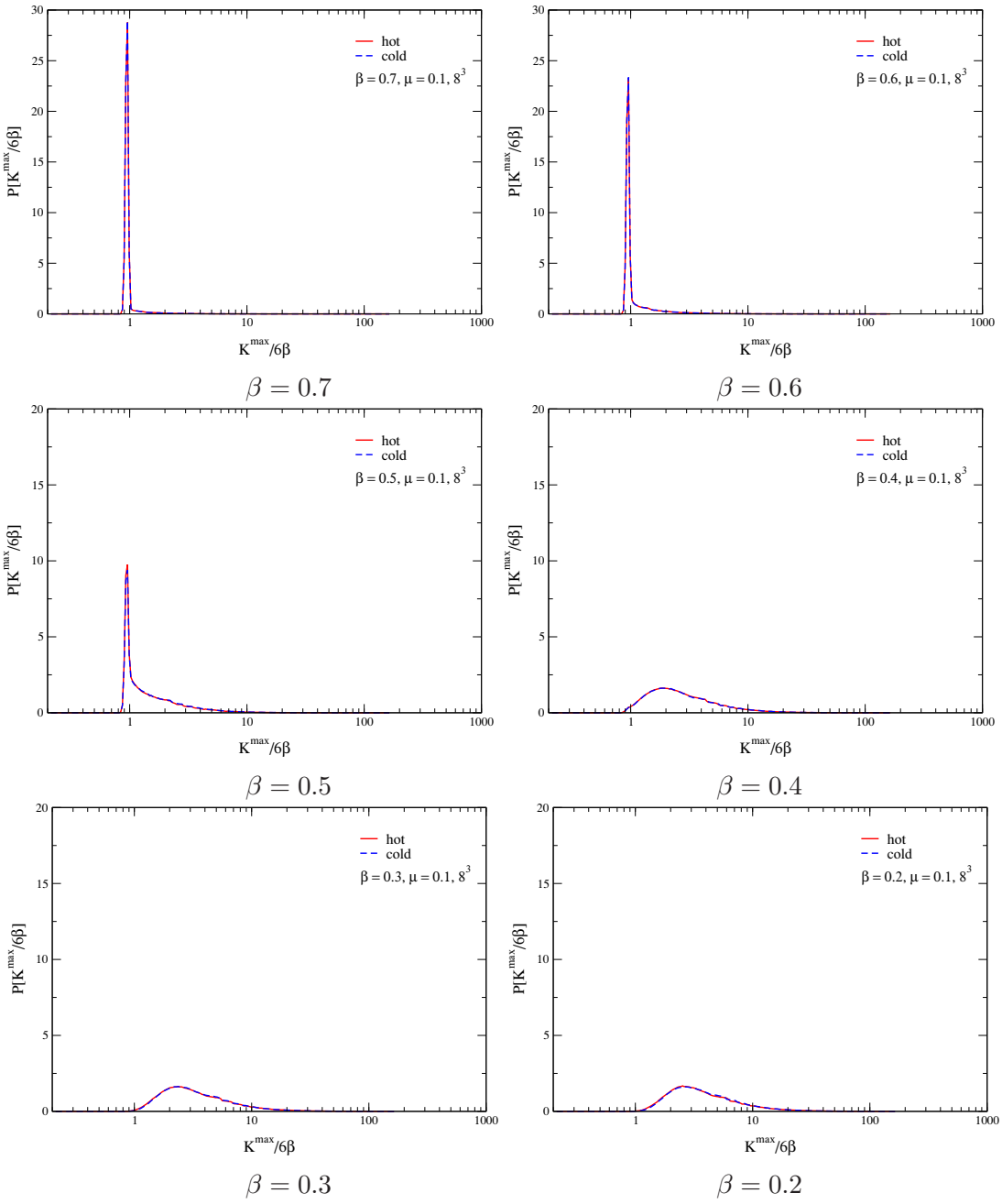

Figure 6. As in the previous figure, for $\mu = 0.1$

lished that the region of failure is strongly correlated with the part of the phase diagram which corresponds to the disordered phase. We have verified that these conclusions do not depend on the lattice volume. Failure at small β values was also observed a long time ago in the case of SU(3) field theory in the presence of static charges [42].

Due to the use of an adaptive stepsize algorithm no runaways or instabilities have been observed. The results we found in the disordered phase are therefore interpreted as convergence to the wrong result. To analyze this, we have studied properties of the

JHEP08(2010)020

dynamics and field distributions in the complexified field space. For the smaller β values, we found that complexified dynamics does not reduce to real dynamics when $\mu = 0$. Furthermore, for the system sizes and parameter values we used, the sign problem is not severe. We conclude therefore that the failure is not due to the presence of the sign problem, but rather due to an incorrect exploration of the complexified field space by the Langevin evolution. The forces appearing in the stochastic process behave very differently at large and small β. Interestingly, in the crossover region at $\beta \approx 0.5$, the dynamics shows a combination of large and small β characteristics. It would be interesting to further understand this, e.g. in terms of competing (nonclassical) fixed points.

We found that several features resemble those found in simulations of simple models with complex noise [53, 68]. Our hope is therefore that a detailed study of simple models with complex noise can shed light on the features observed here with real noise. Such an investigation is currently in progress.

Acknowledgments

We thank Chris Allton and Simon Hands, Debasish Banerjee and Shailesh Chandrasekharan, Philippe de Forcrand, and especially Kim Splittorff, Erhard Seiler and Ion-Olimpiu Stamatescu for discussions. We thank the Blue C Facility at Swansea University for computational resources. This work is supported by STFC.

References

[1] P. de Forcrand, *Simulating QCD at finite density*, PoS(LAT2009)010 [arXiv:1005.0539] [SPIRES].

[2] Z. Fodor and S.D. Katz, *A new method to study lattice QCD at finite temperature and chemical potential*, *Phys. Lett.* **B 534** (2002) 87 [hep-lat/0104001] [SPIRES].

[3] Z. Fodor and S.D. Katz, *Lattice determination of the critical point of QCD at finite T and μ*, *JHEP* **03** (2002) 014 [hep-lat/0106002] [SPIRES].

[4] Z. Fodor and S.D. Katz, *Critical point of QCD at finite T and μ, lattice results for physical quark masses*, *JHEP* **04** (2004) 050 [hep-lat/0402006] [SPIRES].

[5] Z. Fodor, S.D. Katz and K.K. Szabo, *The QCD equation of state at nonzero densities: lattice result*, *Phys. Lett.* **B 568** (2003) 73 [hep-lat/0208078] [SPIRES].

[6] C.R. Allton et al., *The QCD thermal phase transition in the presence of a small chemical potential*, *Phys. Rev.* **D 66** (2002) 074507 [hep-lat/0204010] [SPIRES].

[7] C.R. Allton et al., *The equation of state for two flavor QCD at non-zero chemical potential*, *Phys. Rev.* **D 68** (2003) 014507 [hep-lat/0305007] [SPIRES].

[8] C.R. Allton et al., *Thermodynamics of two flavor QCD to sixth order in quark chemical potential*, *Phys. Rev.* **D 71** (2005) 054508 [hep-lat/0501030] [SPIRES].

[9] R.V. Gavai and S. Gupta, *Pressure and non-linear susceptibilities in QCD at finite chemical potentials*, *Phys. Rev.* **D 68** (2003) 034506 [hep-lat/0303013] [SPIRES].

[10] P. de Forcrand and O. Philipsen, *The QCD phase diagram for small densities from imaginary chemical potential*, *Nucl. Phys.* **B 642** (2002) 290 [hep-lat/0205016] [SPIRES].

JHEP08(2010)020

[11] P. de Forcrand and O. Philipsen, *The QCD phase diagram for three degenerate flavors and small baryon density*, *Nucl. Phys.* **B 673** (2003) 170 [hep-lat/0307020] [SPIRES].

[12] P. de Forcrand and O. Philipsen, *The chiral critical line of $N_f = 2 + 1$ QCD at zero and non-zero baryon density*, *JHEP* **01** (2007) 077 [hep-lat/0607017] [SPIRES].

[13] P. de Forcrand and O. Philipsen, *Constraining the QCD phase diagram by tricritical lines at imaginary chemical potential*, arXiv:1004.3144 [SPIRES].

[14] M. D'Elia and M.-P. Lombardo, *Finite density QCD via imaginary chemical potential*, *Phys. Rev.* **D 67** (2003) 014505 [hep-lat/0209146] [SPIRES].

[15] M. D'Elia and F. Sanfilippo, *The order of the Roberge-Weiss endpoint (finite size transition) in QCD*, *Phys. Rev.* **D 80** (2009) 111501 [arXiv:0909.0254] [SPIRES].

[16] S. Kratochvila and P. de Forcrand, *The canonical approach to finite density QCD*, PoS(LATTICE 2005)167 [hep-lat/0509143] [SPIRES].

[17] A. Alexandru, M. Faber, I. Horvath and K.-F. Liu, *Lattice QCD at finite density via a new canonical approach*, *Phys. Rev.* **D 72** (2005) 114513 [hep-lat/0507020] [SPIRES].

[18] S. Ejiri, *Canonical partition function and finite density phase transition in lattice QCD*, *Phys. Rev.* **D 78** (2008) 074507 [arXiv:0804.3227] [SPIRES].

[19] Z. Fodor, S.D. Katz and C. Schmidt, *The density of states method at non-zero chemical potential*, *JHEP* **03** (2007) 121 [hep-lat/0701022] [SPIRES].

[20] K.N. Anagnostopoulos and J. Nishimura, *New approach to the complex-action problem and its application to a nonperturbative study of superstring theory*, *Phys. Rev.* **D 66** (2002) 106008 [hep-th/0108041] [SPIRES].

[21] J. Ambjørn, K.N. Anagnostopoulos, J. Nishimura and J.J.M. Verbaarschot, *The factorization method for systems with a complex action — A test in random matrix theory for finite density QCD*, *JHEP* **10** (2002) 062 [hep-lat/0208025] [SPIRES].

[22] G. Akemann, J.C. Osborn, K. Splittorff and J.J.M. Verbaarschot, *Unquenched QCD Dirac operator spectra at nonzero baryon chemical potential*, *Nucl. Phys.* **B 712** (2005) 287 [hep-th/0411030] [SPIRES].

[23] K. Splittorff, *Lattice simulations of QCD with $\mu_B \neq 0$ versus phase quenched QCD*, hep-lat/0505001 [SPIRES].

[24] K. Splittorff and J.J.M. Verbaarschot, *Phase of the fermion determinant at nonzero chemical potential*, *Phys. Rev. Lett.* **98** (2007) 031601 [hep-lat/0609076] [SPIRES].

[25] J. Han and M.A. Stephanov, *A random matrix study of the QCD sign problem*, *Phys. Rev.* **D 78** (2008) 054507 [arXiv:0805.1939] [SPIRES].

[26] J.C.R. Bloch and T. Wettig, *Random matrix analysis of the QCD sign problem for general topology*, *JHEP* **03** (2009) 100 [arXiv:0812.0324] [SPIRES].

[27] M.P. Lombardo, K. Splittorff and J.J.M. Verbaarschot, *Distributions of the phase angle of the fermion determinant in QCD*, *Phys. Rev.* **D 80** (2009) 054509 [arXiv:0904.2122] [SPIRES].

[28] M.P. Lombardo, K. Splittorff and J.J.M. Verbaarschot, *The fluctuations of the quark number and of the chiral condensate*, *Phys. Rev.* **D 81** (2010) 045012 [arXiv:0910.5482] [SPIRES].

[29] J. Danzer, C. Gattringer, L. Liptak and M. Marinkovic, *A study of the sign problem for lattice QCD with chemical potential*, *Phys. Lett.* **B 682** (2009) 240 [arXiv:0907.3084] [SPIRES].

JHEP08(2010)020

[30] J.O. Andersen, L.T. Kyllingstad and K. Splittorff, *The sign problem across the QCD phase transition*, *JHEP* **01** (2010) 055 [arXiv:0909.2771] [SPIRES].

[31] S. Hands, T.J. Hollowood and J.C. Myers, *QCD with chemical potential in a small hyperspherical box*, *JHEP* **07** (2010) 086 [arXiv:1003.5813] [SPIRES].

[32] B. Bringoltz, *Large-N spacetime reduction and the sign and silver-blaze problems of dense QCD*, *JHEP* **06** (2010) 076 [arXiv:1004.0030] [SPIRES].

[33] S. Chandrasekharan and U.-J. Wiese, *Meron-cluster solution of a fermion sign problem*, *Phys. Rev. Lett.* **83** (1999) 3116 [cond-mat/9902128] [SPIRES].

[34] M.G. Endres, *Method for simulating $O(N)$ lattice models at finite density*, *Phys. Rev.* **D 75** (2007) 065012 [hep-lat/0610029] [SPIRES].

[35] S. Chandrasekharan, *A new computational approach to lattice quantum field theories*, PoS(LATTICE2008)003 [arXiv:0810.2419] [SPIRES].

[36] D. Banerjee and S. Chandrasekharan, *Finite size effects in the presence of a chemical potential: a study in the classical non-linear $O(2)$ σ-model*, *Phys. Rev.* **D 81** (2010) 125007 [arXiv:1001.3648] [SPIRES].

[37] G. Parisi, *On complex probabilities*, *Phys. Lett.* **B 131** (1983) 393 [SPIRES].

[38] J.R. Klauder, *Stochastic quantization*, in *Recent developments in high-energy physics*, H. Mitter and C.B. Lang eds., Springer-Verlag, Wien Austria (1983) [*J. Phys.* **A 16** (1983) L317] [*Phys. Rev.* **A 29** (1984) 2036].

[39] J.R. Klauder and W.P. Petersen, *Spectrum of certain nonselfadjoint operators and solutions of langevin equations with complex drift*, *J. Stat. Phys.* 39 (1985) 53.

[40] F. Karsch and H.W. Wyld, *Complex langevin simulation of the* SU(3) *spin model with nonzero chemical potential*, *Phys. Rev. Lett.* **55** (1985) 2242 [SPIRES].

[41] J. Ambjørn and S.K. Yang, *Numerical problems in applying the langevin equation to complex effective actions*, *Phys. Lett.* **B 165** (1985) 140 [SPIRES].

[42] J. Ambjørn, M. Flensburg and C. Peterson, *The complex Langevin equation and Monte Carlo simulations of actions with static charges*, *Nucl. Phys.* **B 275** (1986) 375 [SPIRES].

[43] J. Flower, S.W. Otto and S. Callahan, *Complex langevin equations and lattice gauge theory*, *Phys. Rev.* **D 34** (1986) 598 [SPIRES].

[44] E.M. Ilgenfritz, *Complex langevin simulation of chiral symmetry restoration at finite baryonic density*, *Phys. Lett.* **B 181** (1986) 327 [SPIRES].

[45] P.H. Damgaard and H. Huffel, *Stochastic quantization*, *Phys. Rept.* **152** (1987) 227 [SPIRES].

[46] J. Berges and I.O. Stamatescu, *Simulating nonequilibrium quantum fields with stochastic quantization techniques*, *Phys. Rev. Lett.* **95** (2005) 202003 [hep-lat/0508030] [SPIRES].

[47] J. Berges, S. Borsányi, D. Sexty and I.O. Stamatescu, *Lattice simulations of real-time quantum fields*, *Phys. Rev.* **D 75** (2007) 045007 [hep-lat/0609058] [SPIRES].

[48] J. Berges and D. Sexty, *Real-time gauge theory simulations from stochastic quantization with optimized updating*, *Nucl. Phys.* **B 799** (2008) 306 [arXiv:0708.0779] [SPIRES].

[49] G. Aarts and I.-O. Stamatescu, *Stochastic quantization at finite chemical potential*, *JHEP* **09** (2008) 018 [arXiv:0807.1597] [SPIRES].

JHEP08(2010)020

[50] G. Aarts, *Can stochastic quantization evade the sign problem? — The relativistic Bose gas at finite chemical potential*, *Phys. Rev. Lett.* **102** (2009) 131601 [arXiv:0810.2089] [SPIRES].

[51] G. Aarts, *Complex Langevin dynamics at finite chemical potential: mean field analysis in the relativistic Bose gas*, *JHEP* **05** (2009) 052 [arXiv:0902.4686] [SPIRES].

[52] G. Aarts, F.A. James, E. Seiler and I.-O. Stamatescu, *Adaptive stepsize and instabilities in complex Langevin dynamics*, *Phys. Lett.* **B 687** (2010) 154 [arXiv:0912.0617] [SPIRES].

[53] G. Aarts, E. Seiler and I.-O. Stamatescu, *The complex Langevin method: when can it be trusted?*, *Phys. Rev.* **D 81** (2010) 054508 [arXiv:0912.3360] [SPIRES].

[54] C. Pehlevan and G. Guralnik, *Complex Langevin equations and Schwinger-Dyson equations*, *Nucl. Phys.* **B 811** (2009) 519 [arXiv:0710.3756] [SPIRES].

[55] G. Guralnik and C. Pehlevan, *Effective potential for complex Langevin equations*, *Nucl. Phys.* **B 822** (2009) 349 [arXiv:0902.1503] [SPIRES].

[56] H. Nakazato and Y. Yamanaka, *Minkowski stochastic quantization*, *Phys. Rev.* **D 34** (1986) 492 [SPIRES].

[57] A. Roberge and N. Weiss, *Gauge theories with imaginary chemical potential and the phases of QCD*, *Nucl. Phys.* **B 275** (1986) 734 [SPIRES].

[58] N. Prokof'ev and B. Svistunov, *Worm algorithms for classical statistical models*, *Phys. Rev. Lett.* **87** (2001) 160601 [SPIRES].

[59] P. Hasenfratz and F. Karsch, *Chemical potential on the lattice*, *Phys. Lett.* **B 125** (1983) 308 [SPIRES].

[60] M. Campostrini, M. Hasenbusch, A. Pelissetto, P. Rossi and E. Vicari, *Critical behavior of the three-dimensional XY universality class*, *Phys. Rev.* **B 63** (2001) 214503 [cond-mat/0010360] [SPIRES].

[61] T. Banks, R. Myerson and J.B. Kogut, *Phase transitions in abelian lattice gauge theories*, *Nucl. Phys.* **B 129** (1977) 493 [SPIRES].

[62] U. Wenger, *Efficient simulation of relativistic fermions via vertex models*, *Phys. Rev.* **D 80** (2009) 071503 [arXiv:0812.3565] [SPIRES].

[63] P. de Forcrand and M. Fromm, *Nuclear physics from lattice QCD at strong coupling*, *Phys. Rev. Lett.* **104** (2010) 112005 [arXiv:0907.1915] [SPIRES].

[64] U. Wolff, *Simulating the all-order strong coupling expansion III: $O(N)$ sigma/loop models*, *Nucl. Phys.* **B 824** (2010) 254 [*Erratum ibid.* **B 834** (2010) 395] [arXiv:0908.0284] [SPIRES].

[65] J. Langelage and O. Philipsen, *The pressure of strong coupling lattice QCD with heavy quarks, the hadron resonance gas model and the large-N limit*, *JHEP* **04** (2010) 055 [arXiv:1002.1507] [SPIRES].

[66] T.D. . Cohen, *Functional integrals for QCD at nonzero chemical potential and zero density*, *Phys. Rev. Lett.* **91** (2003) 222001 [hep-ph/0307089] [SPIRES].

[67] G. Aarts, unpublished (2009).

[68] G. Aarts, E. Seiler and I.O. Stamatescu, in progress.

JHEP08(2010)020